# Discussion on Finite Size Scaling at Small Volume

Yannick Meurice
The University of Iowa
yannick-meurice@uiowa.edu

DofSB, ANL, April 14, 2009
done in part with A. Bazavov, A. Denbleyker, D. Du, Y. Liu and A. Velytsky

# Outline

1. Discrete aspects of finite size scaling (FSS)

2. Nonlinear effects in $B_4$, the Binder cumulants (0712.1190)

3. The zero volume limit (as a way to learn about the infinite volume limit)

4. $B_4$ for Polyakov's loop in $4D$ $SU(2)$ (universality class?)

5. Finite size effects for the density of states in lattice gauge theory (Phys.Rev.D78:054503)

6. Gap equation for 2D nonlinear sigma models at finite volume (no SB)

# Remarks

This is an informal discussion of several pieces of work in progress articulated around the following question: what can we learn about the critical behavior of lattice models by studying their small volume behavior in a region of parameter space where linear FSS is applicable?

Small lattice systems are easy to simulate or approximate (brute force usually works), but the boundary is not small compared to the bulk.

A RG transformation can be seen as gluing small systems together in order to obtain a new small system of the same size (in the renormalized units)

Irrelevant directions yield corrections of the type (number of sites in one direction)$^{-\omega_i}$ with $\omega_i$ well separated (typically $\omega_i = 1, 3, 5...$). In the linear regime, only a few are important and they can be disentangled.

# Discrete Finite Size Scaling

Consider a lattice model in $D$ dimensions, with lattice spacing $a$, linear size $N$, volume $V = N^D$ and nonlinear scaling variables $u_i$.

Under a RG transformation

$$a \to \ell a;\ N \to N/\ell\ ; u_i \to \ell^{y_i} u_i$$

with $\ell$ a rational value $(N/N')$ (examples: Migdal-Kadanoff or Schrödinger functional)

For scalar models with average magnetization $m$

$$V_{eff}(\ell^{y_m} m, \ell^{y_i} u_i, N/\ell) = \ell^D V_{eff}(m, u_i, N)$$

# Exact Realization: Hierarchical Model

$2^n$ sites Labeled with $n$ indices $x_n, .....x_1$, each index being 0 or 1 (think about a tree with $n$ branching levels).

Kinetic term (sum over blocks of all $2^l$ sizes; not renormalized):

$$S = -\frac{1}{2}\sum_{l=1}^{n}(\frac{c}{4})^l \sum_{x_n,\ldots,x_{l+1}} ( \sum_{x_l,\ldots,x_1} \phi_{(x_n,\ldots,x_1)})^2$$

If $c = 2^{(D-2)/D}$, Gaussian fields scale like in $D$-dimensions

$\ell = 2^{\frac{1}{D}}$: "linear" scale factor (block spin: 2 sites$\rightarrow$1 site). $D = 3$ hereafter

Exact RG transformation affects only the local potential

# Recursion Formula

Initial local measure: $W_0(\phi) = \delta(\phi^2 - 1)$ (Ising) or $W_0(\phi) = e^{-A\phi^2 - B\phi^4}$

Block spin transformation:

$$W_{n+1}(\phi) = C_{n+1} e^{\frac{\beta}{2}(\frac{c}{4})^{n+1}\phi^2} \int d\phi' W_n(\tfrac{(\phi-\phi')}{2}) W_n(\tfrac{(\phi+\phi')}{2}) \ ,$$

Fourier Representation of the RG transformation ($c = 2^{1-2//D}$)

$$R_{n+1}(k) = C_{n+1} exp(-\tfrac{1}{2}\beta \frac{\partial^2}{\partial k^2})(R_n(\tfrac{\sqrt{c}k}{2}))^2$$

$M_n$: the total field $\sum \phi_x$ inside blocks of side $2^n$ ;

$$R_n(k) = \sum_{q=0}^{\infty} \frac{(-ik)^{2q}}{(2q)!} \frac{<(M_n)^{2q}>_n}{(4/c)^{qn}}$$

# 2. Nonlinear effects in Binder cumulants (0712.1190)

We consider the fourth order Binder cumulant

$$B_4 \equiv \frac{< m^4 >}{< m^2 >^2} = f(u_\kappa N^{1/\nu}, u_1 N^{-\omega_1}, u_2 N^{-\omega_2}, \dots)$$

$u_k$ is the relevant scaling variable $u_k \simeq \kappa \equiv (\beta - \beta_c)/\beta_c$ in the linear approximation.

$< m^{2l} >$ are unsubtracted moments of the average spin.

At $\beta_c$ and infinite volume, $B_4$ is a universal quantity.

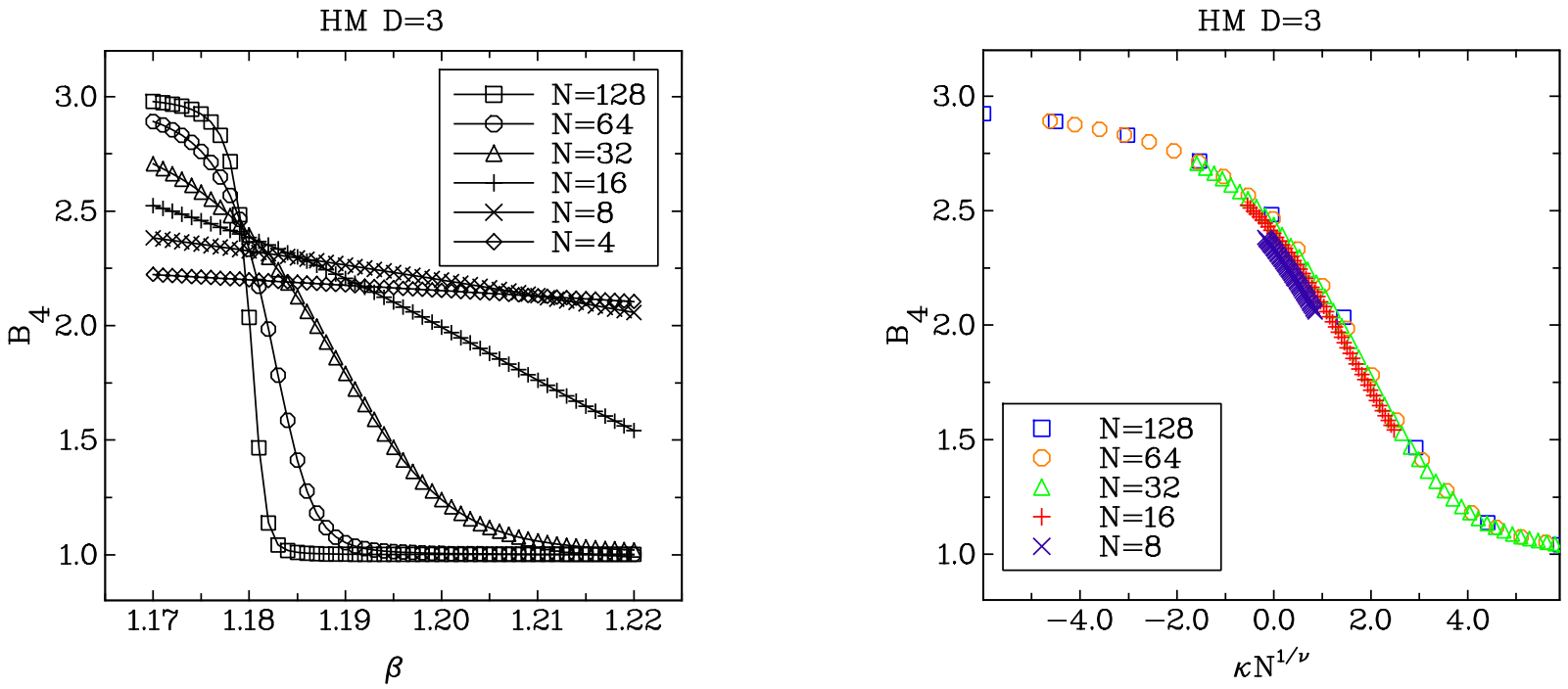


Figure 1: $B_4$ versus $\beta$ (left) and $\kappa N^{1/\nu}$ (right), for $N = 8$, 16, 32, 64 and 128 for the Ising hierarchical model.( $\kappa \equiv (\beta - \beta_c)/\beta_c$).

$$B_4(\beta, N) \simeq B_4(\beta_c, \infty) + f_1 \kappa N^{1/\nu} + f_2 \kappa^2 N^{2/\nu} + (c_0 + c_1 \kappa N^{1/\nu}) N^{-\omega} \ .$$

In the linear approximation ($f_2 = c_1 = 0$), we recover the standard linear FSS formula for the point of intersection denoted $(\beta^\star(N, N'), B_4^\star(N, N'))$ between the two curves $B_4(\beta, N)$ and $B_4(\beta, N')$, namely

$$\begin{aligned} \beta^\star(N, N') &= \beta_c + \beta_c (c_0/f_1) L(N, N') \ , \\ B_4^\star(N, N') &= B_4 + c_0 M(N, N') \ , \end{aligned} \tag{1}$$

with

$$\begin{aligned} L(N, N') &= (N^{-\omega} - N'^{-\omega}) / (N'^{1/\nu} - N^{1/\nu}) \ , \\ M(N, N') &= (N^{-\omega - 1/\nu} - N'^{-\omega - 1/\nu}) / (N'^{1/\nu} - N^{1/\nu}) \ . \end{aligned} \tag{2}$$

# The shrinking interval procedure

In the literature, $B_4$ is often plotted for different volumes but at fixed values of $\beta$. It is better to shrink the interval as the volume increases. Given $N$ and an estimate $\bar{\beta}_c$ of $\beta_c$ from smaller volumes, we should restrict

$$|\beta - \bar{\beta}_c| < \epsilon (f_1/f_2) \bar{\beta}_c N^{-1/\nu} \ .$$

The value of $\epsilon$ needs to be chosen carefully. On one hand, we need $\epsilon$ small enough in order to control the nonlinear effects. On the other hand, if $\epsilon$ is very small, we need a correspondingly good estimate of $\beta_c$. In addition, when $\epsilon$ is too small, the intersections may be far away from the interval.

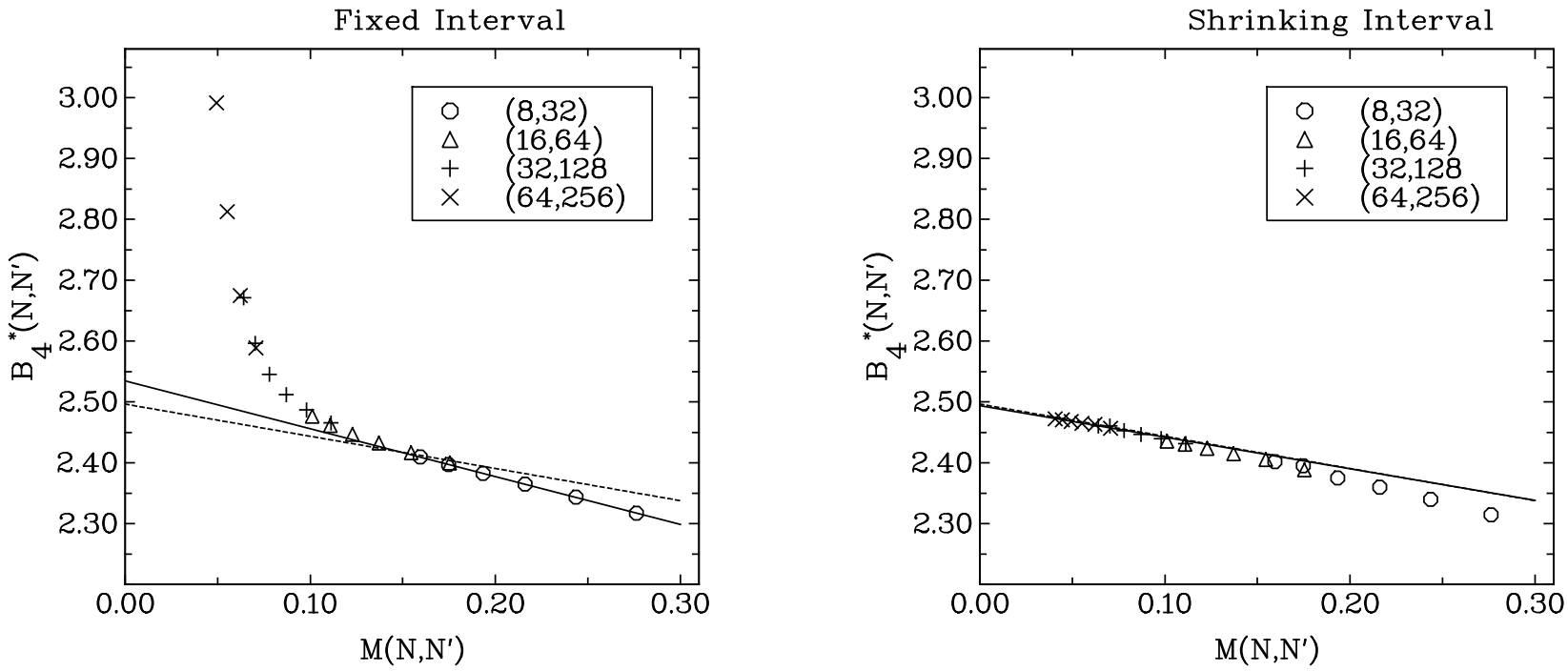


Figure 2: Empirical values of $B_4^\star(N, N')$ versus $M(N, N')$ obtained with the fixed interval procedure (left) and with the shrinking interval procedure (right) for 4 sets of 6 pairs of values. The solid line are linear fits. The dash line is the behavior expected from independent accurate calculations.

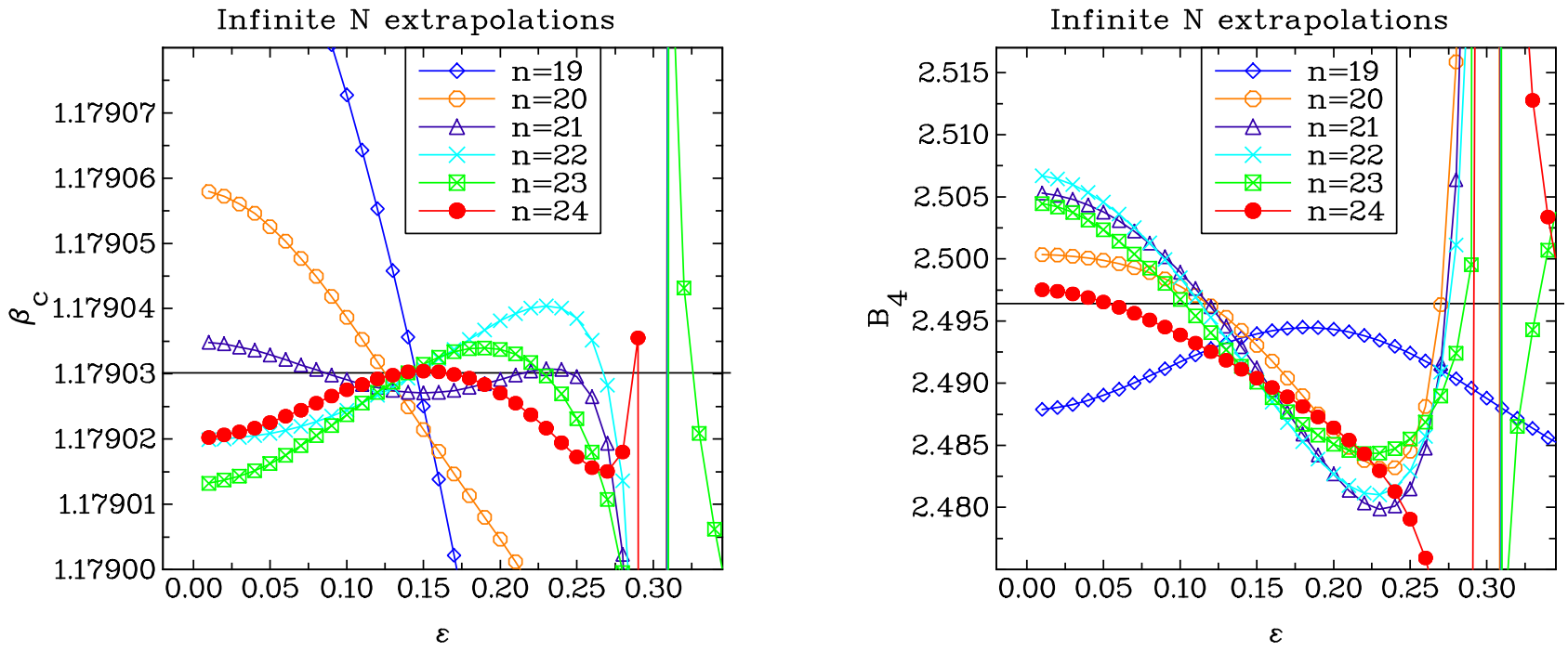


Figure 3: Infinite volume extrapolations of $\beta_c$ and $B_4$ based on 15 point linear fits from the intersections among the $B_4$ curves at $N = 2^{n/3}$ and the 5 values of $N$ immediately below, for $n$ between 19 and 24.

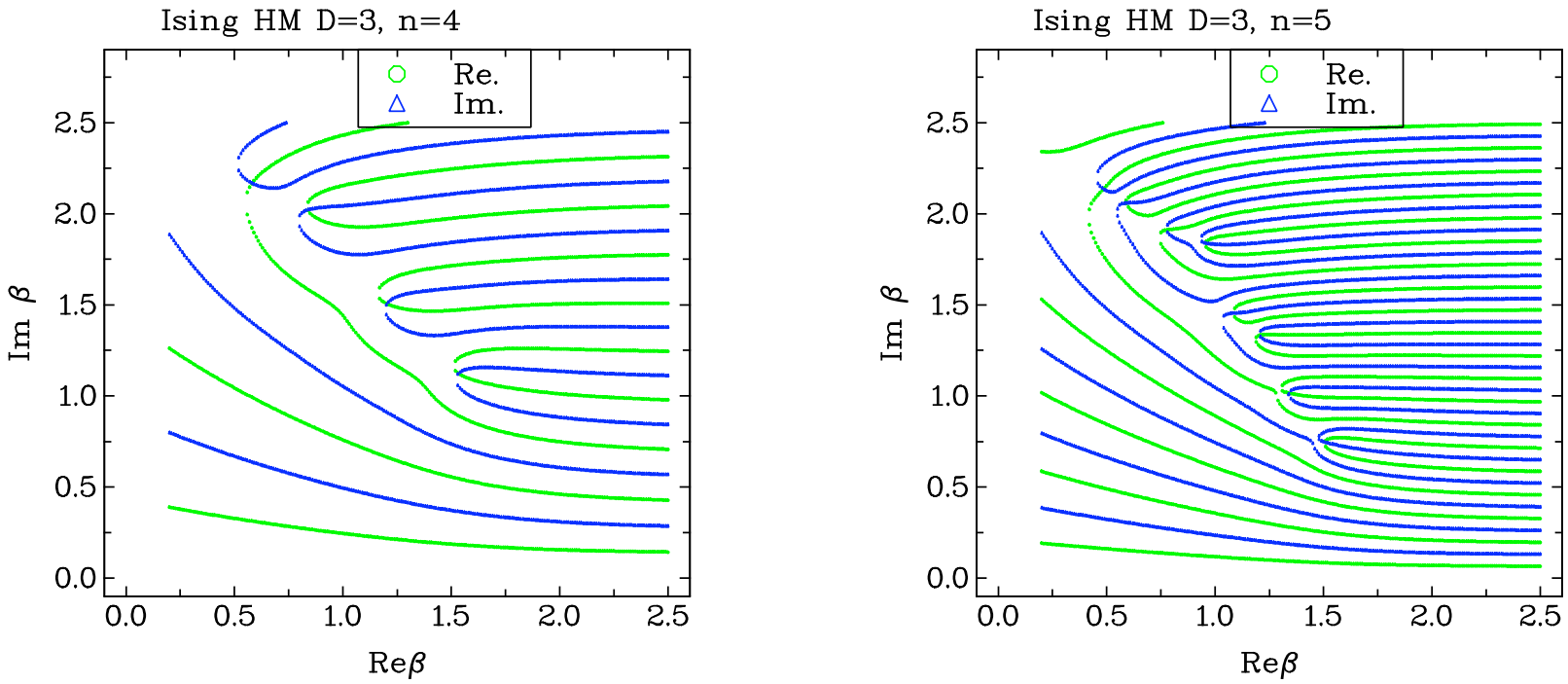


Figure 16: Zeros of the real (green) and imaginary (blue) part of $Z$ for the $D = 3$ Ising HM for $n = 4$ and 5 ($V = 2^n$).

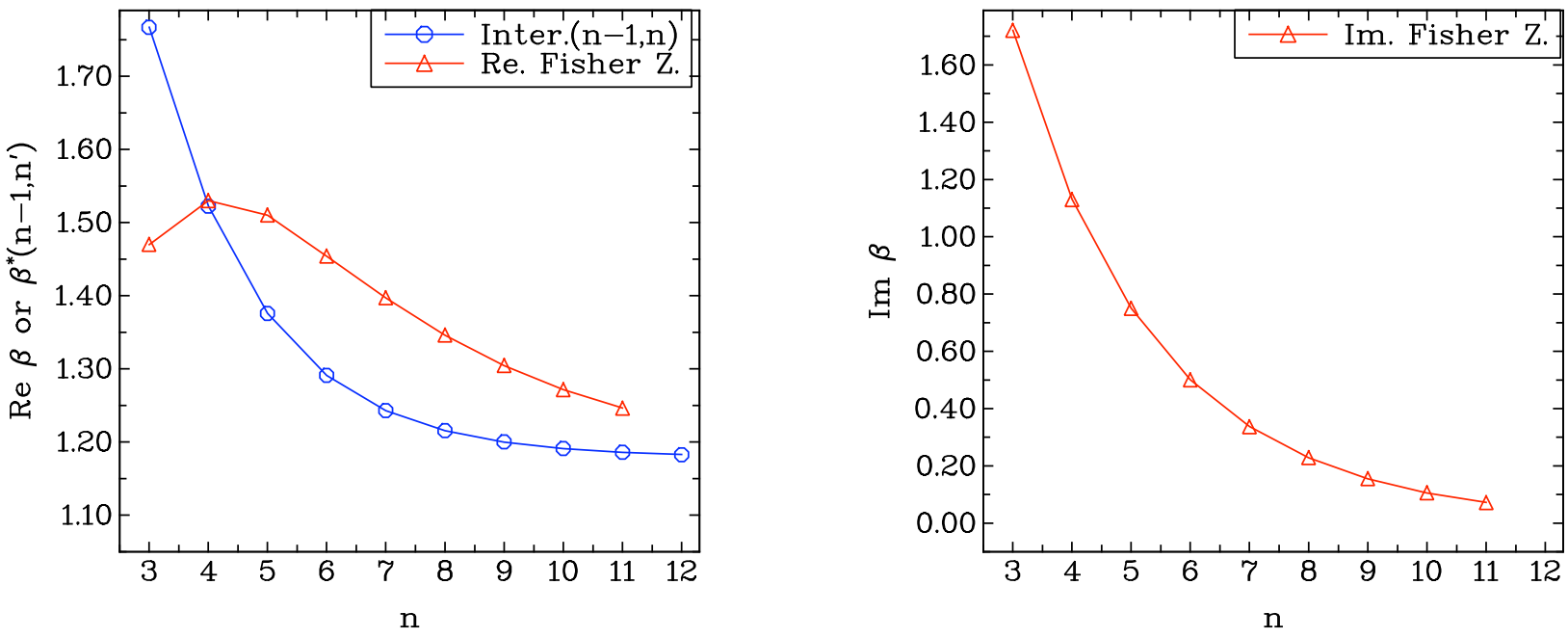


Figure 17: Re and Im part of the zero closest to the real axis compared to the intersections of Binder curves $\beta^\star(n-1,n)$ for $V$ up to $2^{11}$.

# The zero volume limit

$$B_4 = f(u_\kappa N^{1/\nu}, u_1 N^{-\omega_1}, u_2 N^{-\omega_2}, \dots)$$

The $\omega_i$ are widely spaced for the HM

$$\begin{aligned} \omega_1 &= 0.655736 \\ \omega_2 &= 3.17995 \\ \omega_3 &= 5.91212 \end{aligned}$$

A strategy to get accurate estimates at not too large volume is to try to fine tune $u_\kappa$ and $u_1$ to the smallest possible values. Fine tuning $u_1$ can be done by looking for the crossing of the first and second irrelevant directions at very small volume. This was done for a LG measure.

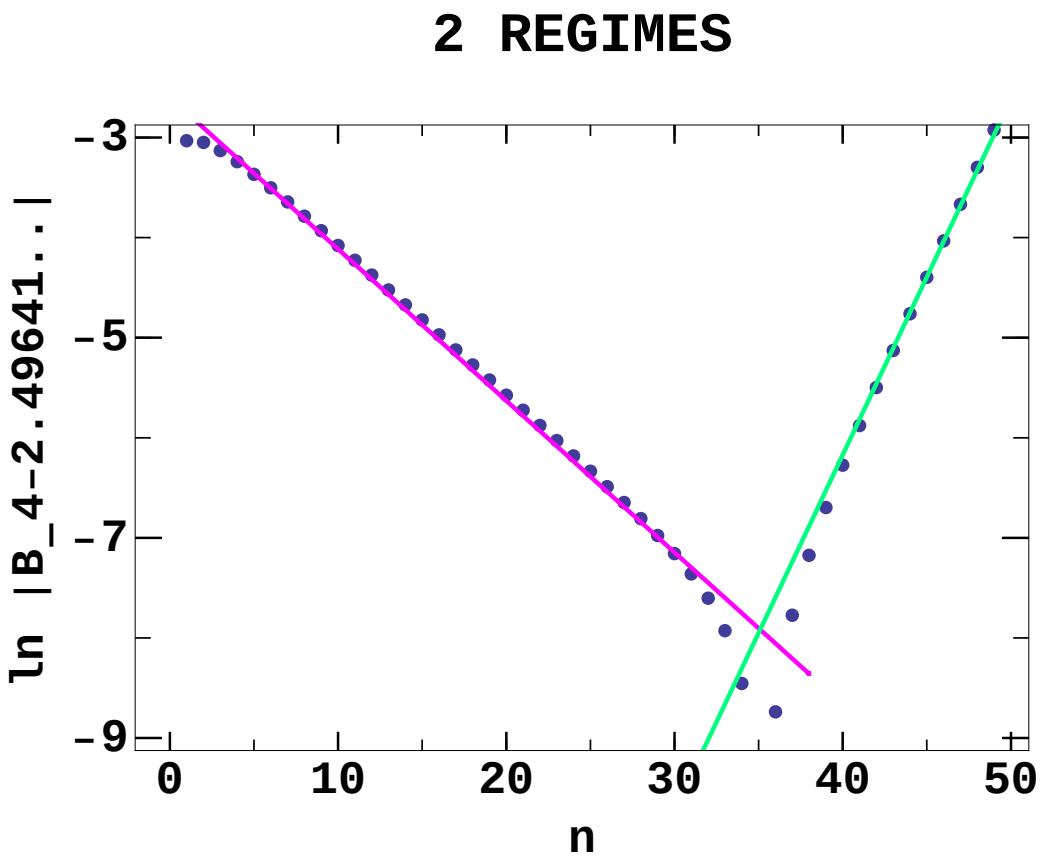


Figure 4: $\ln|B_4 - 2.49641845|$, versus $n = \mathrm{Log}_2 V$. The two lines have slopes corresponding to the first irrelevant direction and the relevant direction (from left to right). $\beta$ was fine tuned with 8 digits.

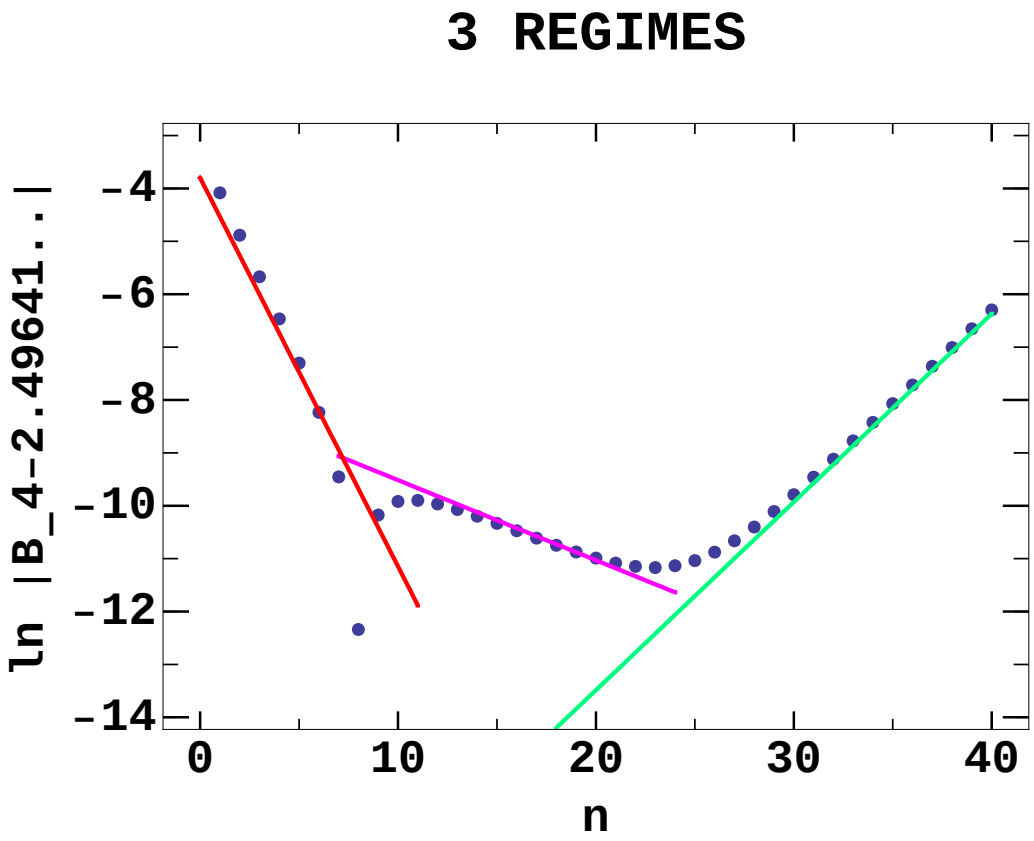


Figure 5: $\ln|B_4 - 2.49641845|$, versus $n = \mathrm{Log}_2 V$. The three lines have slopes corresponding to the second and first irrelevant directions and the relevant direction (from left to right). $\beta$ was fine tuned with 8 digits and $\lambda_4$ with 3 digits.

# Binder cumulants for Polyakov loop in $SU(2)$

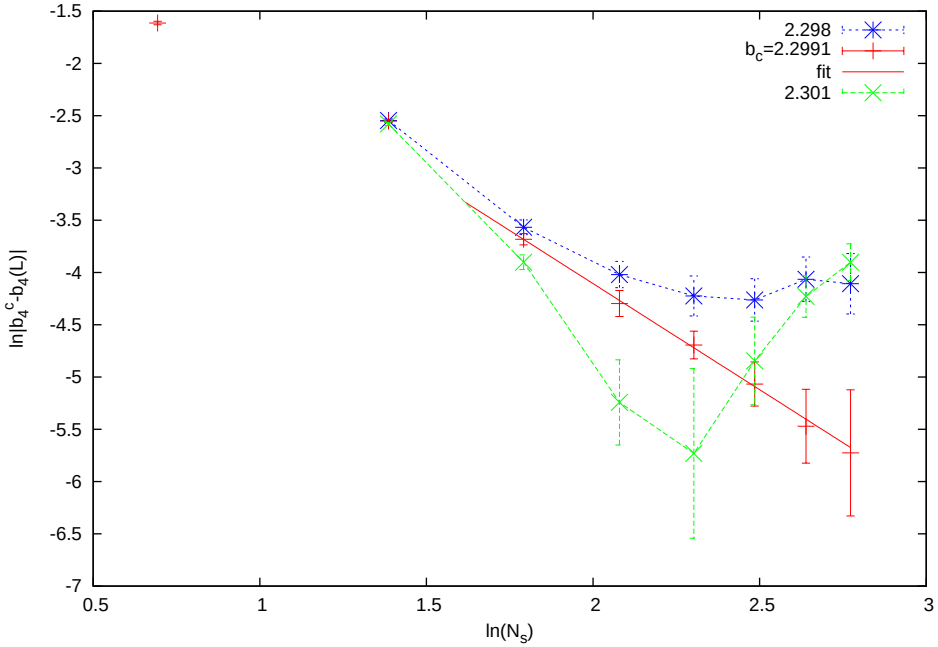


Figure 6: $Ln(|g_4 - g_{4Ising}|)$ versus $Ln(N)$ near $\beta_c$, using A. Velytsky data; linear fit suggests $\omega \simeq 2$ (0.8 expected for Ising)

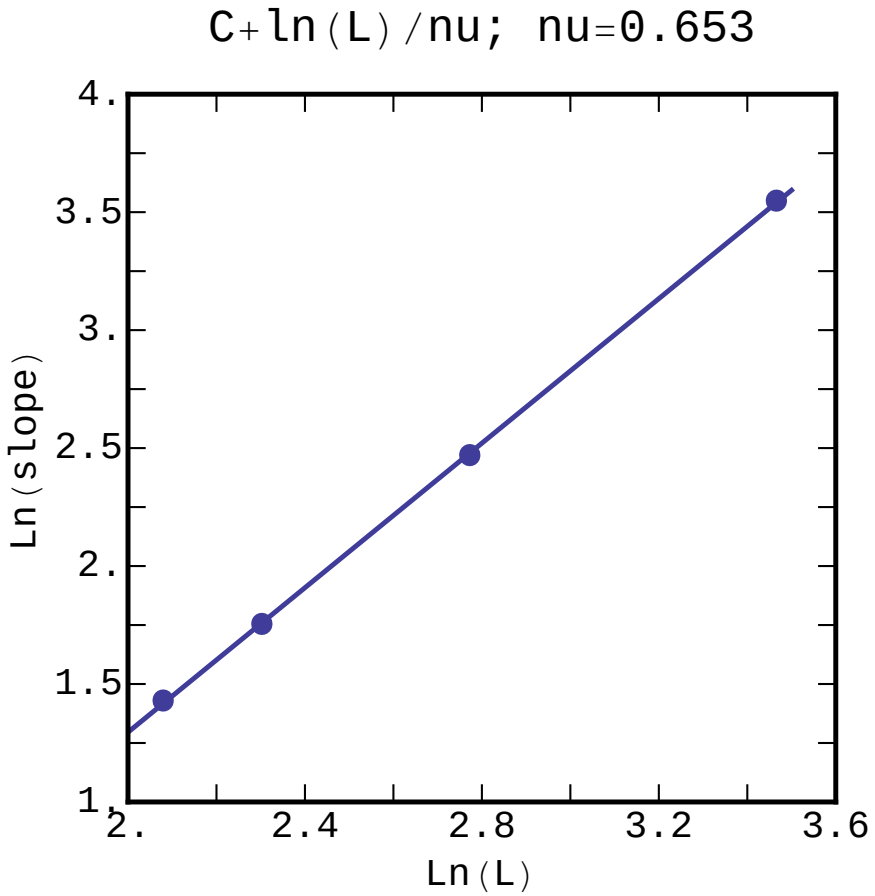


Figure 7: Ln(slope of $g_4$ ) versus $Ln(N)$ near $\beta_c$ at fixed linear size $L$, for $L$= 8, 10, 16 and 32 (from, A. Velytsky data), the slope is 1.531 suggesting $\nu \simeq 0.653$ closer to $O(2)$ than Ising. Error analysis in progress.

# $n(S)$ in Wilson's $SU(2)$ (0807.0185)

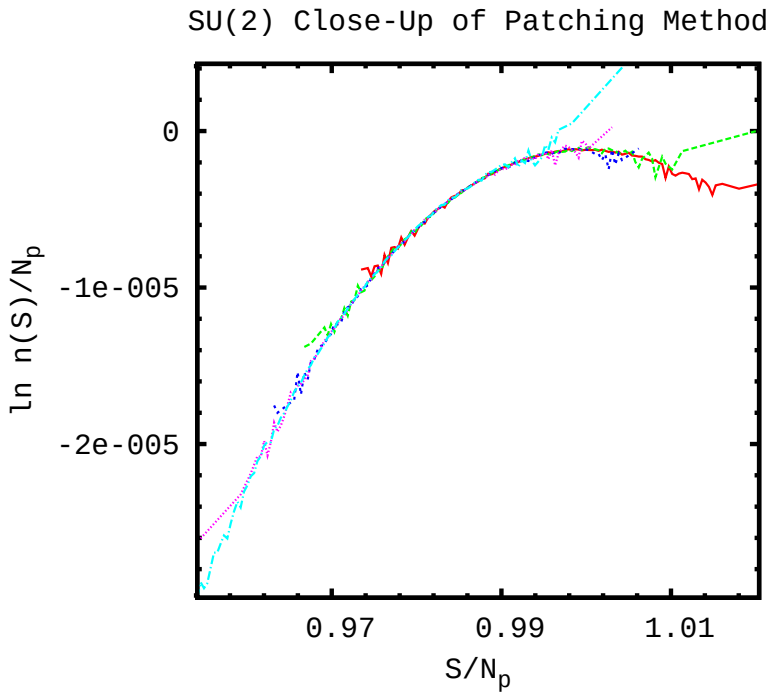


Figure 8: Close-up of the patching process for $6^4$ ($n(S) \propto P_\beta(S)\mathrm{e}^{\beta \mathrm{S}}$).

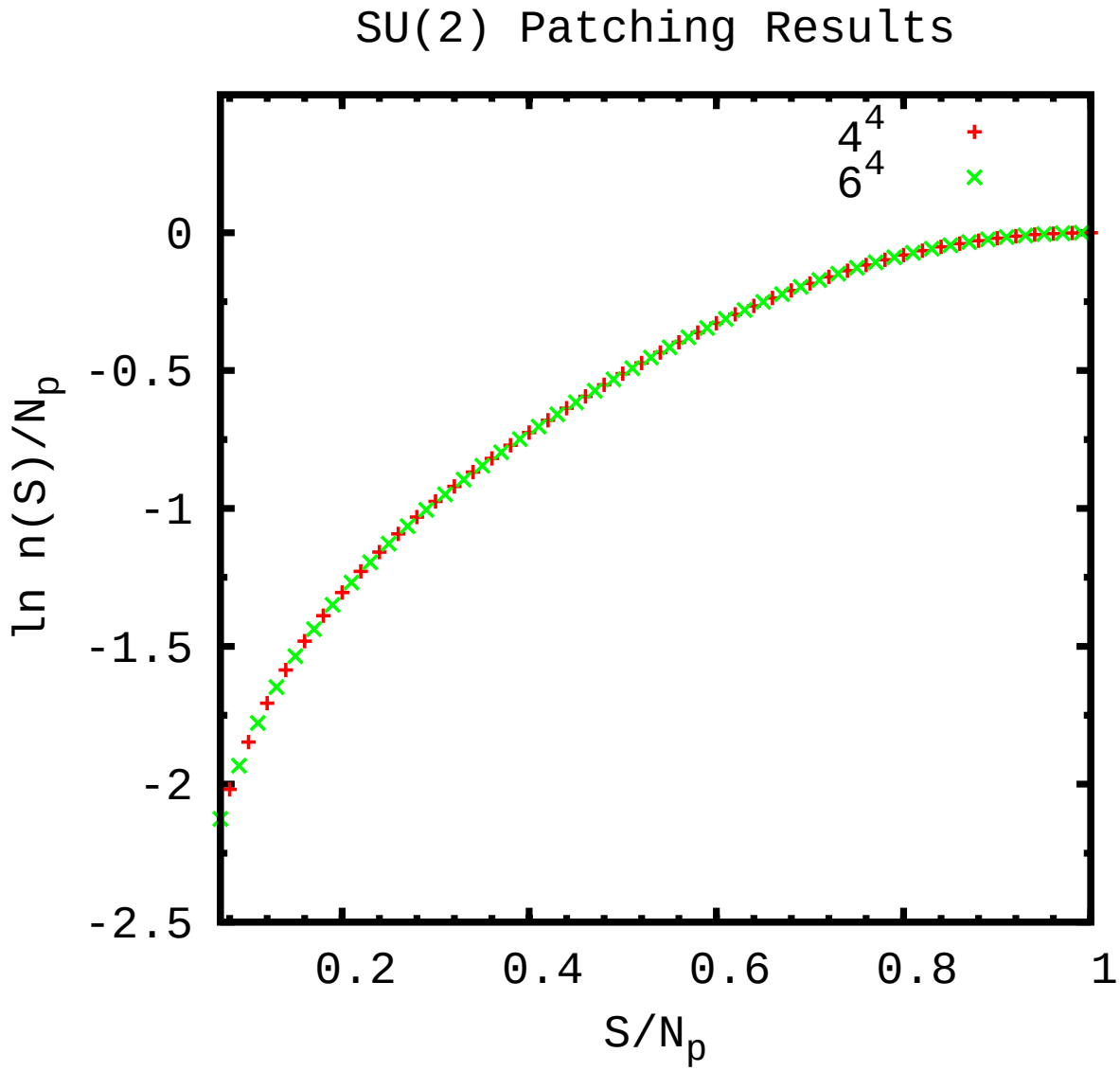




Figure 9: Results of patching for $4^4$ and $6^4$.

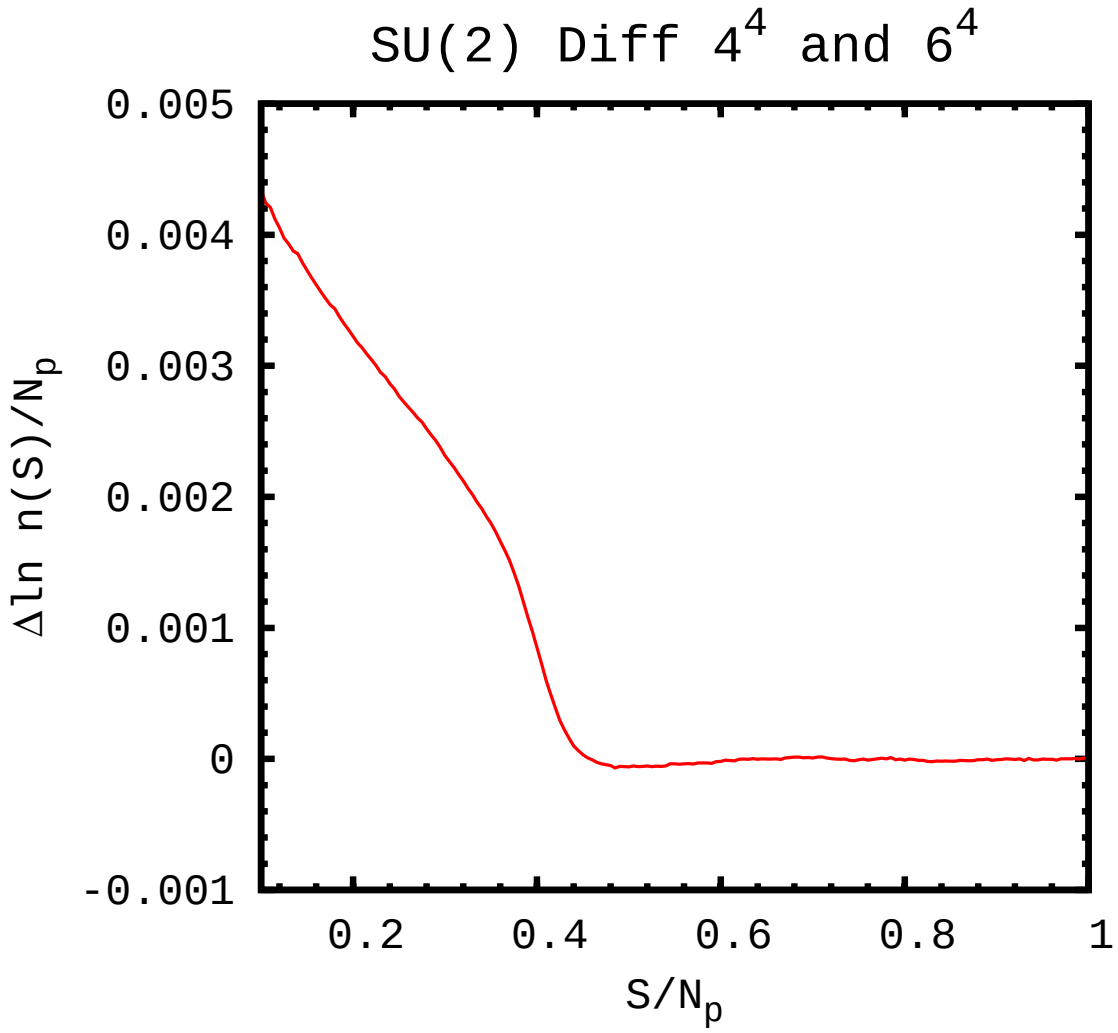


Figure 10: $\Delta \ln n(S)/\mathcal{N}_p$ for $4^4$ and $6^4$.

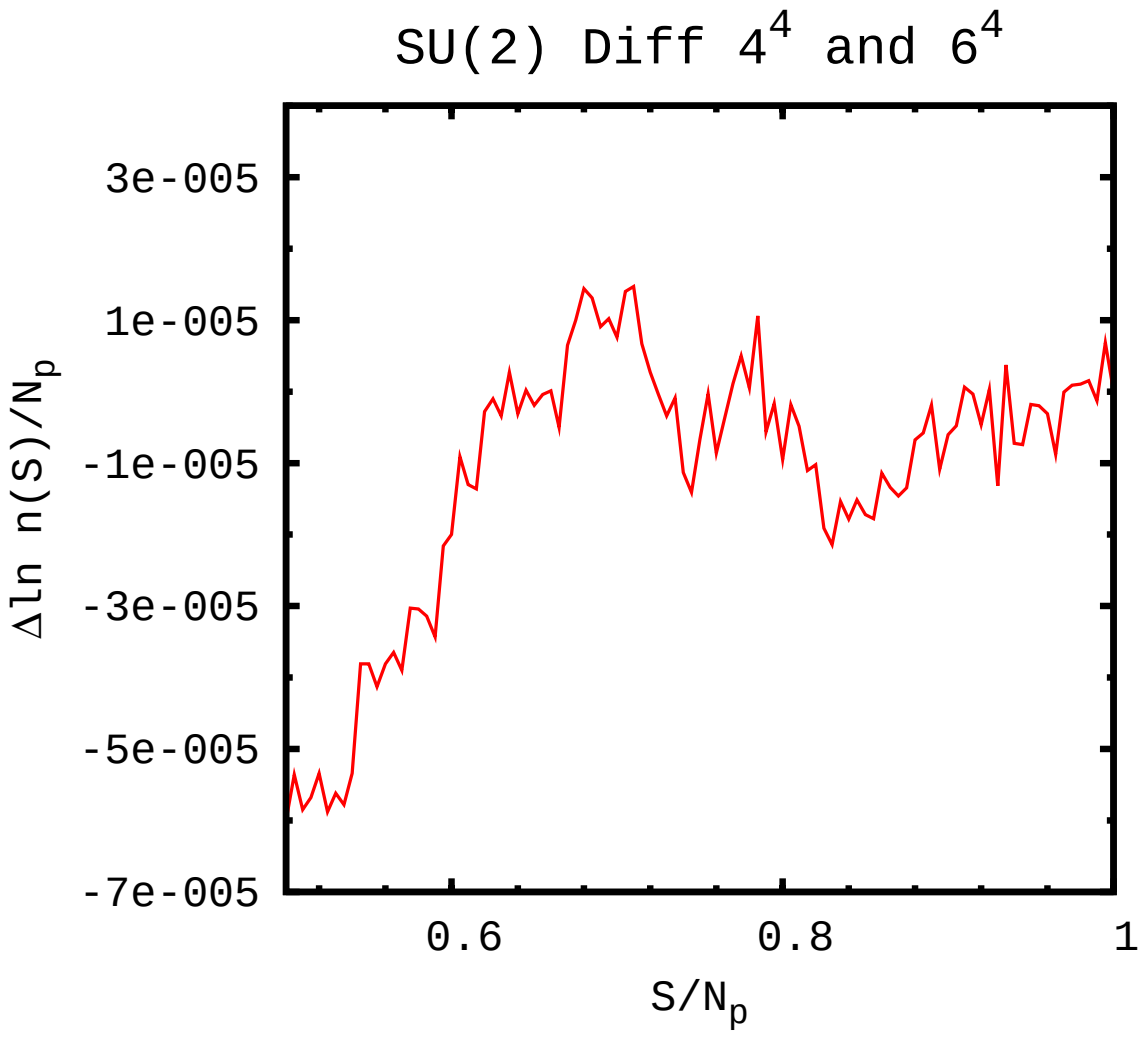


Figure 11: The noise in the tail of $\Delta \ln n(S)/\mathcal{N}_p$ for $4^4$ and $6^4$.

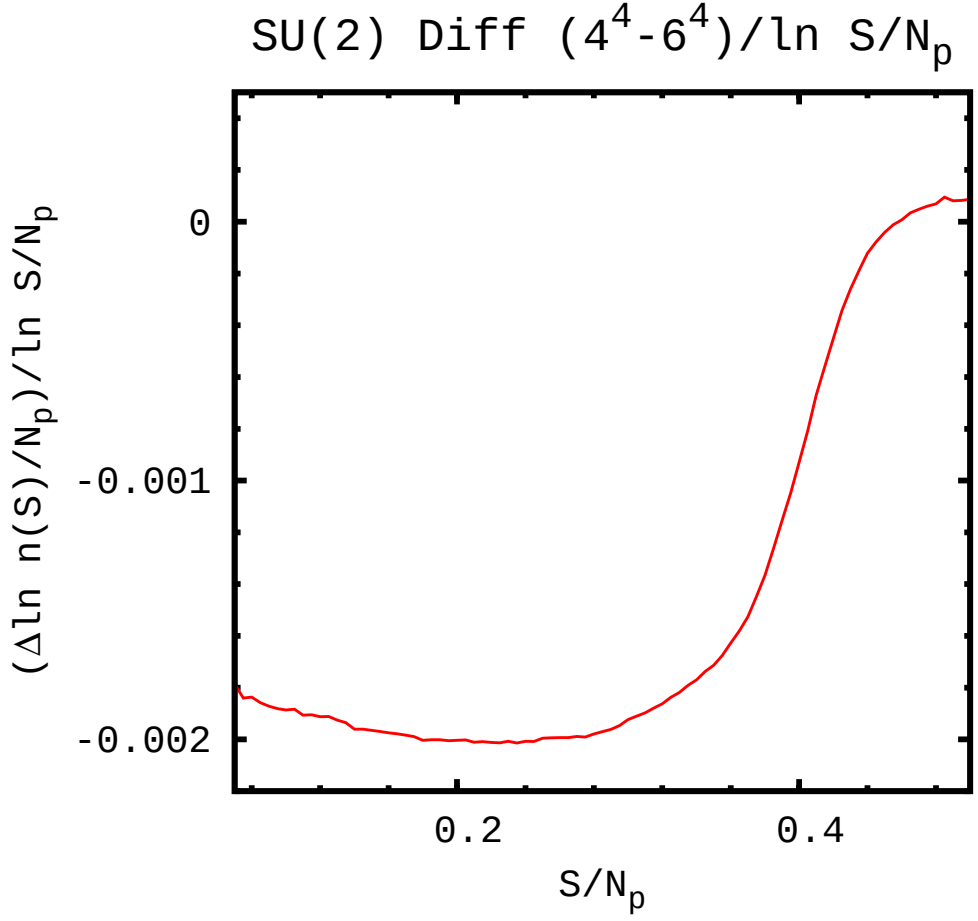


Figure 12: $\Delta \ln n(S)/\mathcal{N}_p$ for $4^4$ and $6^4$ divided by $ln(S/\mathcal{N}_p)$. Predicted constant is -0.0013.

# Fisher's zeros

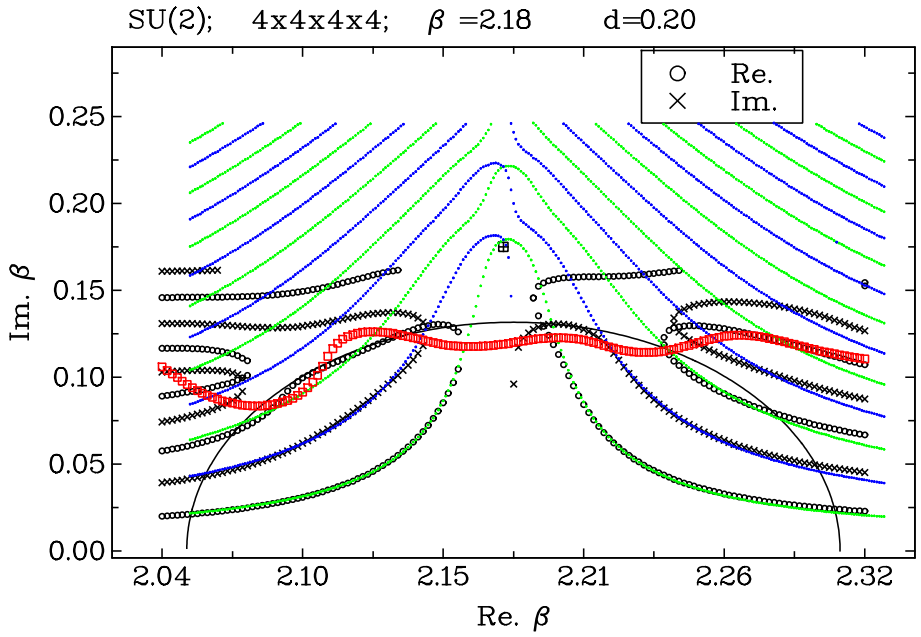


Figure 13: Zeros of the real (crosses) and imaginary (circles) using MC on a $4^4$ lattice, for $SU(2)$ at $\beta_0 = 2.18$. The values for the real (green) and imaginary (blue) parts are obtained from a 4 parameter model.

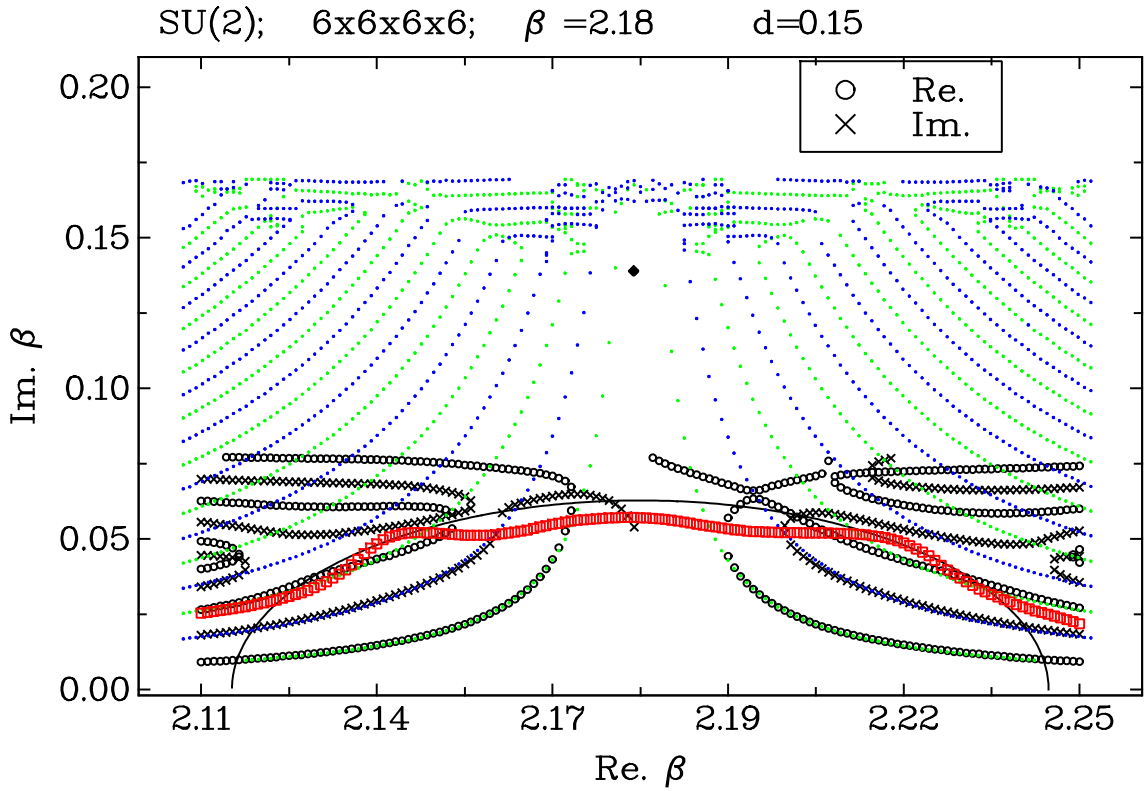


Figure 14: Same for a $6^4$ lattice. The region of confidence for MC shrinks like $V^{-1/2}$.

# With the density of states (D.Du)

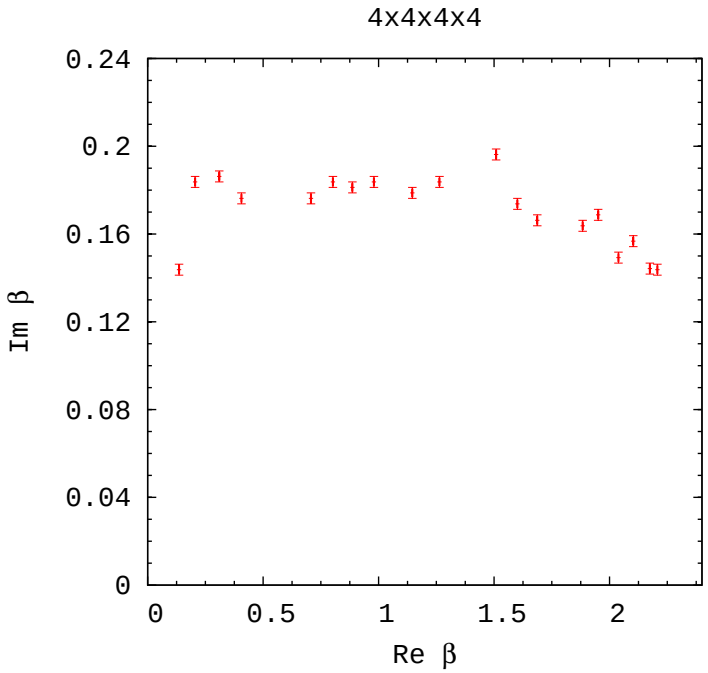


Figure 15: Complex zeros for $SU(2)$ using the density of states for a $4^4$ lattice.

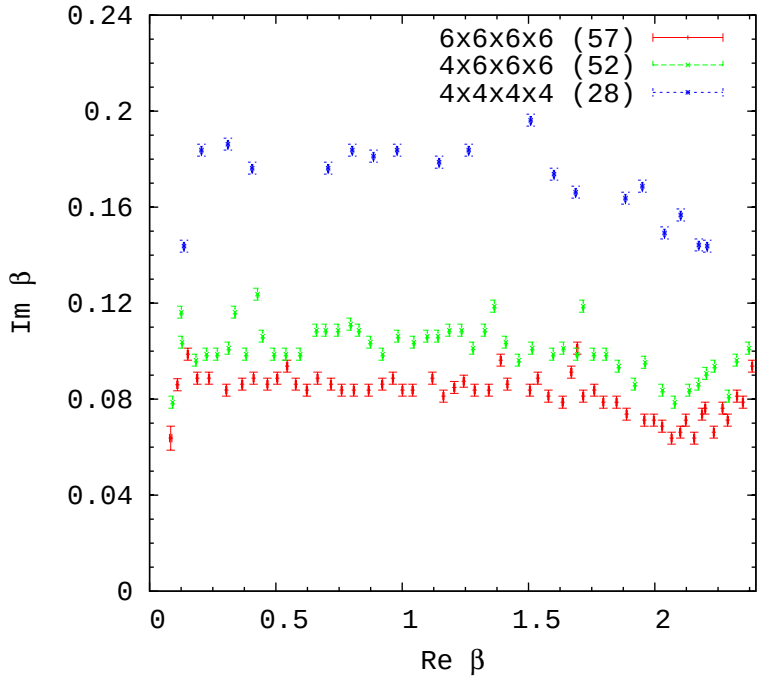


Figure 16: Complex zeros closest to the real axis for $SU(2)$ using the density of states for a $4^4$, $4 \times 6^3$ and $6^4$ lattices (D. Du). $(3/2)^{1.7} \simeq 2$

# $U(1)$ lattice gauge theory

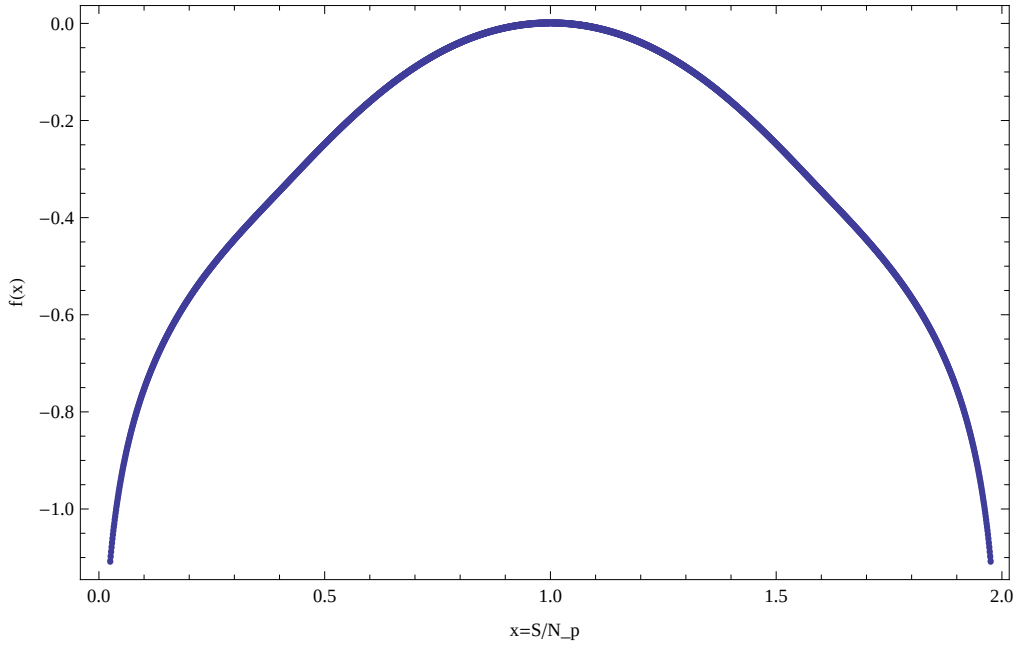


Figure 17: Density of states for $U(1)$ on a $4^4$ lattice by multicanonical methods (A. Bazavov).

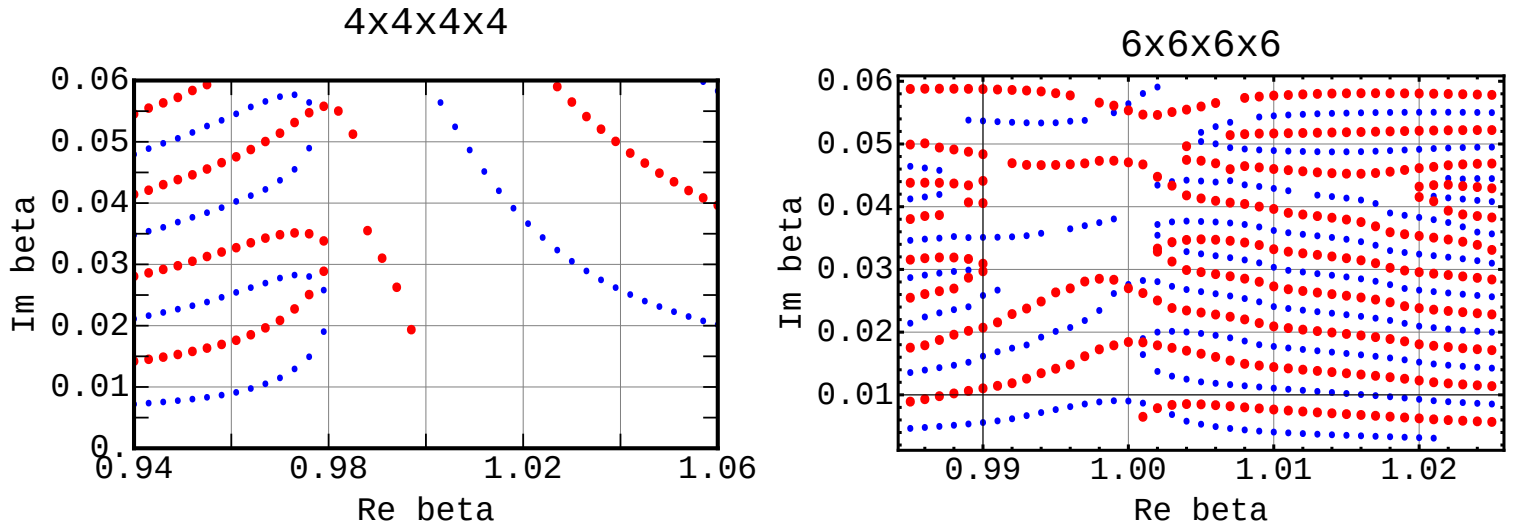


Figure 18: Zeros of Re and Im part of $Z$ for $U(1)$ using the density of states for $4^4$ and $6^4$ lattices.

# Nonlinear $O(N)$ sigma model on a square lattice

$$Z = \int \prod_x d^N \phi_x \delta(\vec{\phi}_x \vec{\phi}_x - 1)\ \mathrm{e}^{-(1/g_0^2) E[\{\phi\}]}$$

with $E[\{\phi\}] = \sum_{x,e} (1 - \vec{\phi}_x \vec{\phi}_{x+e})$

We assume a cubic lattice with an even number of sites in each directions and periodic boundary conditions. Under these conditions (as for $SU(2N)$ LGT)

$$Z[-g_0^2] = \mathrm{e}^{4DL^D/g_0^2} Z[g_0^2]$$

This can be seen by changing variable $\phi \longrightarrow -\phi$ on sublattices with lattice spacing twice larger and such that they share exactly one site with each link of the original lattice.

# Gap equation

$$\prod_{j=1}^{D} \int_{-\pi}^{\pi} \frac{dk_j}{2\pi} \frac{1}{2(\sum_{j=1}^{D}(1-\cos(k_j))+M^2} = 1/\lambda^t$$

with $\lambda^t = g_0^2 N$ kept constant as $N$ becomes large.

The saddle point equation is invariant under $\lambda^t \to -\lambda^t$ together with $M^2 \to -M^2 - 4D$. This can be seen by changing variables $k_j \to k_j + \pi$ for all $j$.

For $D = 2$, $\lambda^t \to 0$ when $M^2 \to \ 0, \ -8 \ , -4 \pm i\epsilon$ with double poles at $(k_1, k_2) = (0,0), \ (\pi,\pi), \ (0,\pi), \ (0,\pi)$ respectively.

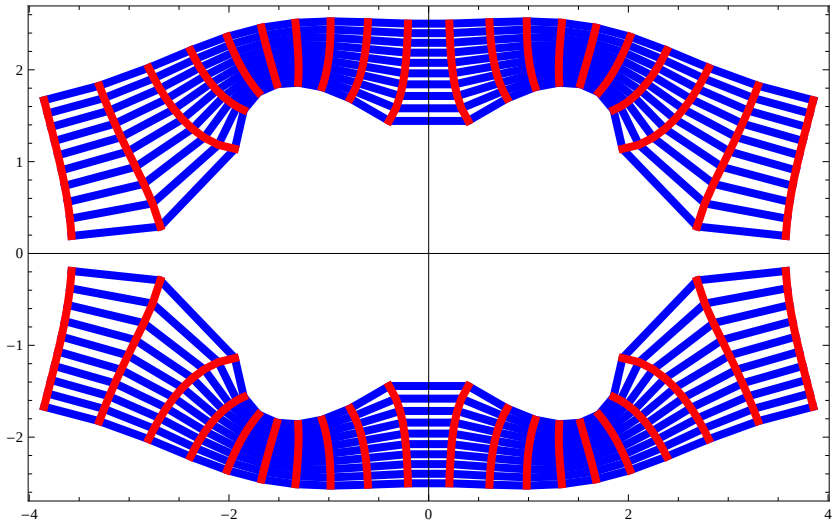


Figure 19: Complex values taken by $\lambda^t$ when $M^2$ varies over the complex plane (here on horizontal and vertical lines in the $M^2$ plane).

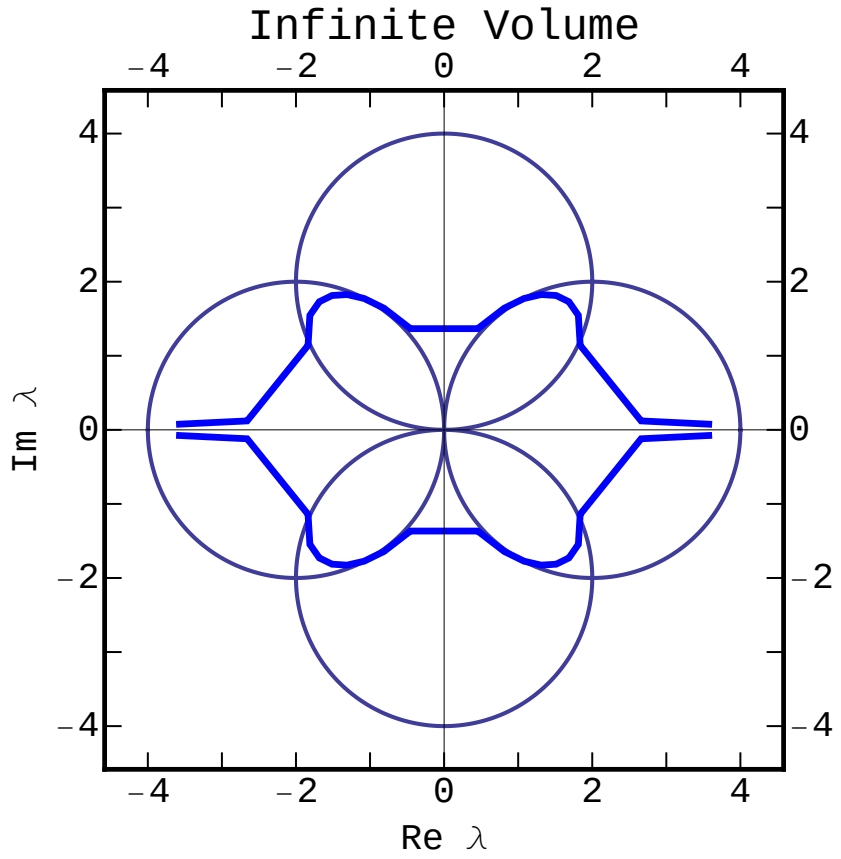


Figure 20: Complex values taken by $\lambda^t$ when $M^2$ varies over the complex plane (here on horizontal and vertical lines in the $M^2$ plane); the circles are inverses of the asymptotic lines in the $1/\lambda^t$ plane.

# Finite Volume

On a $L \times L$ lattice, $k_i = 0, \frac{2\pi}{L}, 2\frac{2\pi}{L}, \ldots (L-1)\frac{2\pi}{L}$

The gap equation becomes: $\sum_{k_1,k_2} \frac{1}{2(\sum_{j=1}^{D}(1-\cos(k_j))+M^2}} = 1/\lambda^t$

The maping becomes a rational function: $\lambda^t = \frac{P(M^2)}{Q(M^2)}$

Singular points ($\frac{\partial \lambda^t}{\partial M^2} = 0$) when $P'Q - PQ' = 0$

As $V = L \times L$ increases, the singular points move toward $[-8, 0]$.

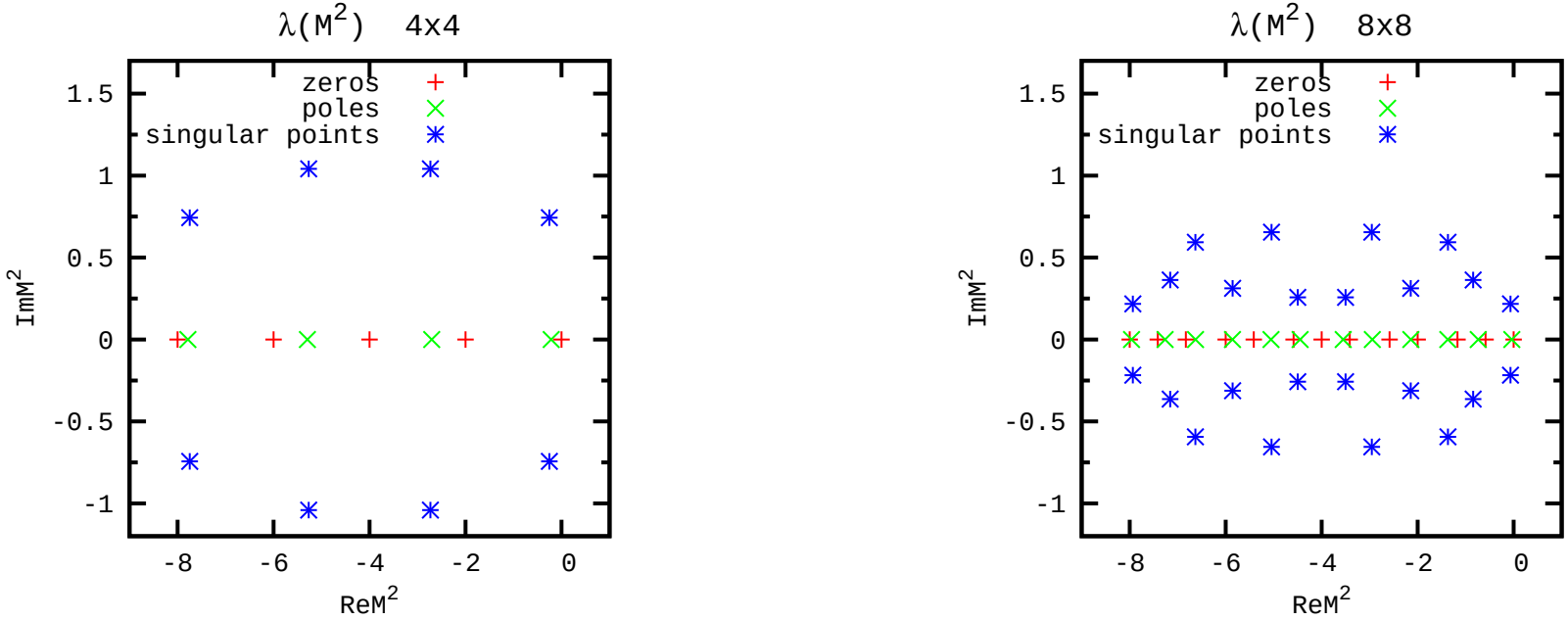


Figure 21: Zeros, poles and singular points of $\lambda(M^2)$ in the $M^2$ plane for 4x4 and 8x8 latices.

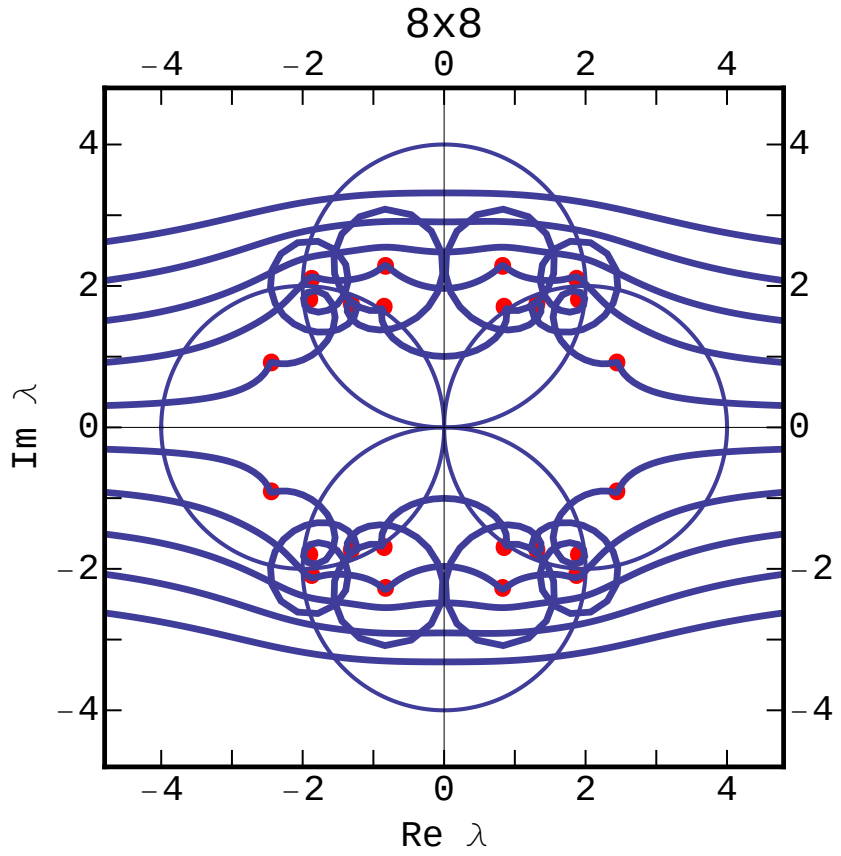


Figure 22: Images in the $\lambda$ plane of lines of constant imaginary part 2.25, 1.75, 1.25, 0.75, 0.25, -0.25, ....,-2.25 and of the singular points (red dots) for a 8x8 lattice Zeros , poles and singular points in the $M^2$ plane for a 8x8 latice.

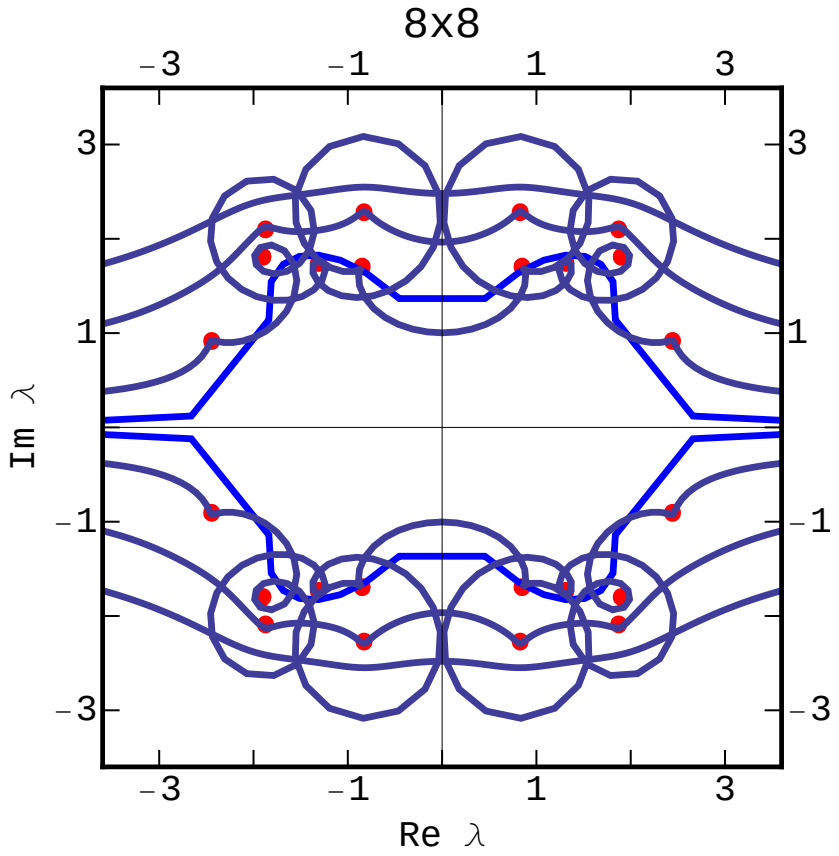


Figure 23: Images in the $\lambda$ plane of lines of constant imaginary part and of the singular points (red dots) for a 8x8 lattice. Inside line is at infinite volume.

# Conclusions

- Nonlinear effects should be carefully estimated before trying to do accurate calculations of Binder cumulants.
- Irrelevant directions should be studied at small volume.
- Universality class for $SU(2)$ finite T transition is not obviously Ising (but should be).
- Volume effects under control for the density of states of Wilson action.
- Large-N 2D sigma models: no SB at complex coupling (the inside of the "clover") in the complex $\lambda^t$ plane corresponds to Riemann sheets in the $M^2$ plane.